Optical Coherence Tomography Intensity Correlates with Extracellular Matrix Components in the Airway Wall

Carpaij, Orestes A; Goorsenberg, Annika W M; d'Hooghe, Julia N S; de Bruin, Daniel M; van den Elzen, Richard M; Nawijn, Martijn C; Annema, Jouke T; van den Berge, Maarten; Bonta, Peter I; Burgess, Janette K

Published in:
American Journal of Respiratory and Critical Care Medicine

DOI:
10.1164/rccm.201908-1512LE

Publication date:
2020

Optical Coherence Tomography Intensity Correlates with Extracellular Matrix Components in the Airway Wall

Orestes A. Carpaij MD[1,2*$], Annika W.M. Goorsenberg MD[3*], Julia N.S. d'Hooghe MD PhD[3], Daniel M. de Bruin PhD[4], Richard M. van den Elzen[4], Martijn C. Nawijn PhD[1,5], Jouke T. Annema MD PhD[3], Maarten van den Berge MD PhD[1,2], Peter I. Bonta MD PhD[2#], Janette K. Burgess PhD[1,5#]

*Both authors contributed equally to this work

#Both authors share last authorship

$ Corresponding author: o.a.carpaij@umcg.nl, work address: Hanzeplein 1, 9713 GZ Groningen, department of pulmonology and tuberculosis, AA11.

1. University of Groningen, University Medical Center Groningen, Groningen Research Institute for Asthma and COPD (GRIAC), Groningen, The Netherlands.
2. University of Groningen, University Medical Center Groningen, Department of Pulmonology, Groningen, The Netherlands.
3. Amsterdam UMC, University of Amsterdam, Department of Respiratory Medicine, Amsterdam, The Netherlands.
4. Amsterdam UMC, University of Amsterdam, Department of Biomedical Engineering & Physics, Amsterdam, The Netherlands.
5. University of Groningen, University Medical Center Groningen, Department of Pathology and Medical Biology, Groningen, The Netherlands.

Contributions

Conception and design: JH, DD, RE, PB, JA, JB

Analysis and interpretation: OC, AG, JH, DD, RE, MN, MB, DD, RE, PB, JA, JB

Drafting the manuscript: OC, AG

Revising it critically for important intellectual content: MN, MB, PB, JK

AJRCCM Articles in Press. Published April 30, 2020 as 10.1164/rccm.201908-1512LE

Non-Author Contributors: TB, MJ, JV, KS, JR, OB, TD

Funding statement

The department of respiratory medicine of Amsterdam UMC received a grant for material support from St Jude Medical. This study was funded by the Dutch Lung Foundation (grant number 5.2.13.064JO), The Netherlands Organization for Health Research and Development (grant number 90713477) and Stichting Astma Bestrijding (grant number SAB 2018/041). Funders were not involved in data collection, analysis, decision to publish or preparation of the manuscript. This project is co-financed by the Ministry of Economic Affairs and Climate Policy by means of the PPP Allowance made available by the Top Sector Life Sciences & Health to stimulate public-private partnerships. J.K.Burgess was funded by a Rosalind Franklin Fellowship provided by the University of Groningen and the European Union.

AJRCCM Articles in Press. Published April 30, 2020 as 10.1164/rccm.201908-1512LE

To the editor,

Obstructive pulmonary diseases are characterised by structural airway remodeling, including alterations in extracellular matrix (ECM) [1]. The ECM profile differs between asthmatic and non-asthmatic airways, with less elastin, and higher abundance of collagen I and fibronectin in asthma [2]. Additionally, increased airway wall collagen deposition is associated with more severe disease in asthma [3]. In COPD, alterations in collagen and elastin affect the mechanical properties of the lung, subsequently decreasing lung elasticity and contributing to emphysema [1]. Currently, two diagnostic tools are available to assess airway remodeling: thorax computed tomography and endobronchial biopsies. While bronchial wall thickness and lumen area can be assessed by computed tomography, the resolution is insufficient to assess separate airway wall layers and ECM components, leaving the pathophysiology of airway wall remodeling unclear. Biopsies are the gold standard for determining airway remodeling; however, the applicability is limited due to its invasiveness, small sample area and elaborative histology processing.

Optical coherence tomography (OCT) generates high resolution, real-time, near-infrared-based cross-sectional images of the airway wall [4,5], with potential for visualizing airway remodeling and enabling 3D reconstructions. Several studies found an increased airway wall thickness and decreased lumen area in asthma and COPD patients using OCT [5,6]. Furthermore, OCT imaging was able to identify and quantify mucosal and submucosal airway layers [4]. To the best of our knowledge, no study has linked OCT imaging to ECM protein deposition in the airway wall. We hypothesized that the ECM deposition within the airway wall can be detected using OCT. The aim of this study was to relate the OCT scattering characteristics with ECM deposition in the airway wall.

Data were acquired as previously described [4]. The medical ethics committee of the AMC approved the protocol (NL51605.018.14) and informed consent was obtained. In brief, five patients scheduled for a lobectomy were included. From these five lobectomies, thirteen airways were dissected and marked with needles to match ex-vivo OCT images with histological sections. Ex-vivo OCT imaging was performed immediately after resection, using a C7 Dragonfly from St Jude Medical (St Paul, MN, USA). The OCT images were analysed using Matlab software (Natick MA, USA), which enabled roll-off correction and point spread function as previously described [7]. Three sequential frames were combined to minimize noise. Sheath and lumen segmentation were applied according to Adams *et al.* to minimize the influence

AJRCCM Articles in Press. Published April 30, 2020 as 10.1164/rccm.201908-1512LE

of scattering intense components in the lumen [8]. OCT areas were calculated using a threshold in light scattering intensity, illustrated in **figure 1**. To correct for probe optics and the imperfect sampling of the OCT system in depth, the fixed threshold was adjusted for the probe's distance to the airway wall in each axial line: a lower threshold was used in longer distances and vice versa. Within each calculated OCT area, the median OCT intensity was measured.

The histological sections were stained with Picosirius Red (TC; total collagen), Masson's Trichrome blue (MT blue; total collagen, bone), anti-collagen A1 antibody (CA1; collagen type 1 A1), Verhoeff's (EL; elastin) and anti-fibronectin antibody (FN; fibronectin). The region of interest (ROI) was defined as the area of the airway wall between the epithelium and the outer border of the desmin-positive smooth muscle. Sections without distortions within the ROI were included. The stained sections for each airway were aligned and colour deconvoluted using ImageJ [9]. Thereafter, the positive area and mean grayscale of the stained airway wall were calculated (threshold of >150 and mean of 0 – 255 grayscale intensity respectively). Associations were tested using linear mixed effects model with intercept per subject.

For *in vitro* experiments, 1x1x3cm plastic containers were printed with a 3D printer, then filled with 0,5ml 5% Gelatin methacrylamide (GelMA) and 0,5% Lithium acylphosphinate (LAP) photo-initiator, containing $1x10^6$ primary lung fibroblasts/ml. The gels were polymerized by UV light (405nm, 2x2 minutes). On one side of the container a droplet of 50µl containing 4,7mg Bovine Serum Albumin (BSA, Sigma Aldrich, the Netherlands), 4,7mg Elastin peptides (Biorbyt, UK), or 4,7mg/ml CA1 (Rat-tail Collagen I, Germany) was applied. These droplets were mixed with 5% GelMA and polymerized, covered by 0,5ml 5% GelMA cell-mixture, and polymerized again. The container was subsequently perforated in order to insert the OCT probe. OCT images were captured, starting at the position where the proteins were added, followed by GelMA without proteins, and ending outside the container.

A total of 36 from the 51 OCT-histology pairs from the right upper lobe and left lower lobe were analysed. Reasons for exclusion were damaged histology sections (7 pairs), unavailability for additional staining, (6 pairs) and OCT images of airway bifurcations (2 pairs). The mean lumen area of the included sections was 2.38 (±2.06) mm^2. ECM component stained areas showed a similar spatial pattern as the OCT threshold measured area **(figure 1)**. Quantification of ECM component stained areas were positively correlated with the OCT area, while MT blue mean grayscale also correlated with OCT intensity **(table 1)**.

AJRCCM Articles in Press. Published April 30, 2020 as 10.1164/rccm.201908-1512LE

In the *in vitro* studies, CA1 and elastin were detected using OCT, while BSA was not detected. (**figure 2**). In the absence of exogenous protein no OCT signal was observed in the hydrogel.

This study shows for the first time that OCT is able to detect and quantify ECM protein deposition in the airway wall. In other research areas focusing on skin and ovarian tissue, an association has been made between collagen deposition and OCT imaging [10,11]. In the airways however, OCT imaging studies have mainly focused on the identification and quantification of the airway wall structure. Intriguingly, elastin and fibronectin area correlated the strongest with OCT area, yet no significance was found between intensity parameters.

Our findings that OCT may directly reflect ECM deposition, without the need of extracting biopsies is of interest in obstructive lung diseases in which airway remodeling plays an important role. Furthermore, by assessing not only thickness but also ECM content of the airway wall, it might be possible to monitor treatments targeting airway remodeling in more detail, such as bronchial thermoplasty and liquid nitrogen spray.

An achievement of this study is the development of an automated analysis of the OCT image and light scattering intensity areas by threshold and segmentation technique. While in previous studies OCT areas were drawn manually, this study shows that a light scattering–based intensity threshold can be used to automatically identify and quantify ECM structures. Additionally, by combining this method with innovative polarization sensitive - OCT systems, it may be possible to analyse individual structural components of the airway wall with even greater accuracy [12].

A limitation needs to be addressed: in order to make a comparison between OCT and histology we used ex-vivo material. However, by using this approach we were able to assess ECM structures of the entire airway wall in a cross sectional manner, which would not be possible in-vivo. Despite this, a strong correlation between OCT light scattering areas and ECM stained components within the airways was found, which was validated in our *in vitro* studies.

In conclusion, our data shows that increased OCT intensity areas correspond to and correlate with higher ECM abundance in the airway wall. This suggests that it is possible to directly measure airway remodeling *in vivo*, in a minimally invasive, real-time manner.

AJRCCM Articles in Press. Published April 30, 2020 as 10.1164/rccm.201908-1512LE

Acknowledgements

We would like to thank T. Borghuis and M.R. Jonker for excellent technical assistance and Klaas Sjollema from the University Medical Center Groningen Microscopy and Imaging Center for assistance with image analysis. The authors would also like to acknowledge and thank J.J.T.H. Roelofs, O. de Boer and T. Dirksen from the pathology department, Amsterdam UMC, for their committed and professional work. Last, we would like to thank J.M. Vonk of the Epidemiology department of the University Medical Center Groningen for her statistical assistance.

AJRCCM Articles in Press. Published April 30, 2020 as 10.1164/rccm.201908-1512LE

Figure 1 legend

Three airway wall ECM staining sections aligned to the paired OCT-image. The upper panel shows the OCT image and matched histology sections, the lower panel shows the corresponding OCT threshold image and histology sections after color deconvolution. ***OCT****: optical coherence tomography image after sheath and lumen segmentation (blue line), showing the area above the threshold (threshold adjusted per axial line for the distance between the lumen and the airway wall) in red,* ***TC****: total collagen,* ***CA1****: collagen A1,* ***EL****: elastin, all three stained sections with the area above the threshold (i.e. >150 of 255 grayscale) in black.*

Figure 2 legend

OCT images of plastic containers filled with ***cells*** *(0,5ml 5% GelMA, 0,5% LAP),* ***BSA*** *(including a droplet of 50µl of 4,7mg BSA),* ***Elastin*** *(including 50µl of 4,7mg elastin peptides), and* ***Collagen I*** *(including 50µl of 4,7mg Rat-tail collagen). A: protein containing area, B: GelMA without protein, C: OCT probe leaving the container, D: OCT probe outside the container, E: boundary between different layers, F: plastic container reflection, G: measured OCT signal.*

AJRCCM Articles in Press. Published April 30, 2020 as 10.1164/rccm.201908-1512LE

References

1 Ito JT, Lourenço JD, Righetti RF, *et al.* Extracellular Matrix Component Remodeling in Respiratory Diseases: What Has Been Found in Clinical and Experimental Studies? *Cells* 2019;**8**:342.

2 Vignola AM, Kips J, Bousquet J. Tissue remodeling as a feature of persistent asthma. *J Allergy Clin Immunol* 2000;**105**:1041–53.

3 Benayoun L, Druilhe A, Dombret M-C, *et al.* Airway structural alterations selectively associated with severe asthma. *Am J Respir Crit Care Med* 2003;**167**:1360–8. doi:10.1164/rccm.200209-1030OC

4 D'Hooghe JNS, Goorsenberg AWM, De Bruin DM, *et al.* Optical coherence tomography for identification and quantification of human airway wall layers. *PLoS One* 2017;**12**:1–13.

5 Ding M, Chen Y, Guan WJ, *et al.* Measuring Airway Remodeling in Patients With Different COPD Staging Using Endobronchial Optical Coherence Tomography. *Chest* 2016;**150**:1281–90. doi:10.1016/j.chest.2016.07.033

6 Hariri LP, Adams DC, Applegate MB, *et al.* Distinguishing tumor from associated fibrosis to increase diagnostic biopsy yield with polarization-sensitive optical coherence tomography. *Clin Cancer Res* 2019;:clincanres.0566.2019.

7 Freund JE, Faber DJ, Bus MT, *et al.* Grading upper tract urothelial carcinoma with the attenuation coefficient of in-vivo optical coherence tomography. *Lasers Surg Med* 2019;**51**:399–406.

8 Adams DC, Pahlevaninezhad H, Szabari M V, *et al.* Automated segmentation and quantification of airway mucus with endobronchial optical coherence tomography. *Biomed Opt Express* 2017;**8**:4729–41.

9 Schneider CA, Rasband WS, Eliceiri KW. NIH Image to ImageJ: 25 years of image analysis. *Nat Methods* 2012;**9**:671–5.

10 Ud-Din S, Foden P, Stocking K, *et al.* Objective assessment of dermal fibrosis in cutaneous scarring: using optical coherence tomography, high frequency ultrasound and immuno-histo-morphometry of human skin. *Br J Dermatol* 2019;:0–2.

AJRCCM Articles in Press. Published April 30, 2020 as 10.1164/rccm.201908-1512LE

11 Yang Y, Wang T, Biswal NC, *et al.* Optical scattering coefficient estimated by optical coherence tomography correlates with collagen content in ovarian tissue. *J Biomed Opt* 2011;**16**:090504.

12 Feroldi F, Davidoui V, Gräfe M, *et al.* In vivo multifunctional optical coherence tomography at the periphery of the lungs. *Biomed Opt Express* 2019;**May**.

AJRCCM Articles in Press. Published April 30, 2020 as 10.1164/rccm.201908-1512LE

Table 1: regression coefficients paired OCT-histology areas and intensities

	Optical Coherence Tomography area (mm^2)		Optical Coherence Tomography intensity (arbitrary unit)	
	B-value (95% CI)	P-value	B-value (95% CI)	P-value
Total collagen area (mm^2)	**0.39 (0.22 – 0.57)**	**7.3×10^{-5}**	-	-
Total collagen mean grayscale	-	-	0.97 (-0.14 – 2.08)	8.3×10^{-2}
Masson's Trichrome blue area (mm^2)	**0.42 (0.23 – 0.62)**	**1.4×10^{-4}**	-	-
Masson's Trichrome blue mean grayscale	-	-	**0.58 (0.09 – 1.08)**	**2.3×10^{-2}**
Collagen A1 area (mm^2)	**028 (0.09 – 0.48)**	**5.8×10^{-3}**	-	-
Collagen A1 mean grayscale	-	-	0.19 (-0.89 – 1.26)	7.0×10^{-2}
Elastin area (mm^2)	**0.70 (0.39 – 1.01)**	**2.8×10^{-4}**	-	-
Elastin mean grayscale	-	-	0.48 (-0.68 – 1.63)	4.1×10^{-1}
Fibronectin area (mm^2)	**0.49 (0.12 – 0.86)**	**1.1×10^{-2}**	-	-
Fibronectin mean grayscale	-	-	0.32 (-0.53 – 1.16)	4.5×10^{-1}

AJRCCM Articles in Press. Published April 30, 2020 as 10.1164/rccm.201908-1512LE

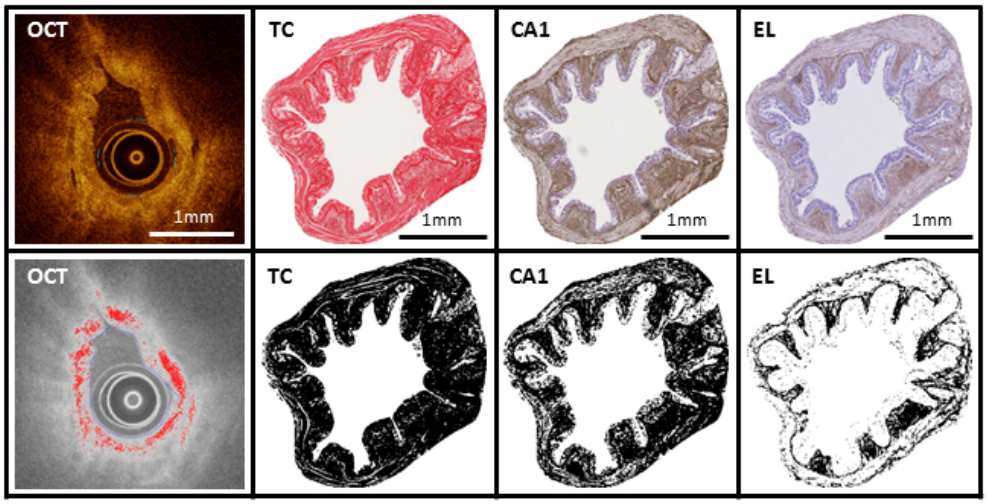

Figure 1

173x88mm (96 x 96 DPI)

AJRCCM Articles in Press. Published April 30, 2020 as 10.1164/rccm.201908-1512LE

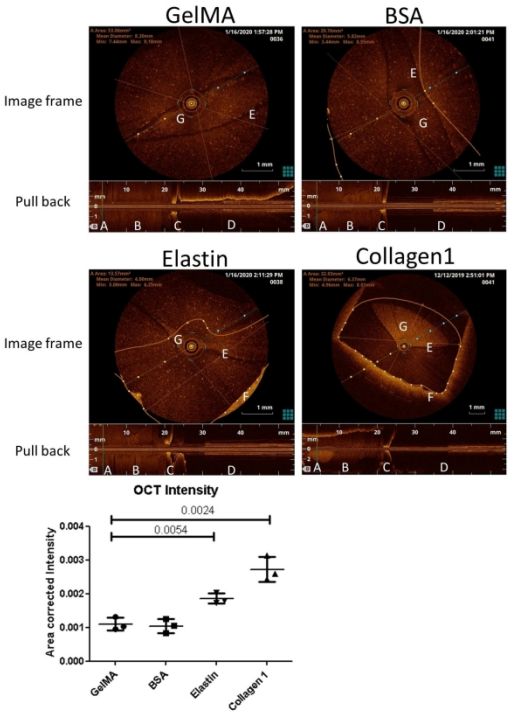

Figure 2

253x190mm (300 x 300 DPI)

AJRCCM Articles in Press. Published April 30, 2020 as 10.1164/rccm.201908-1512LE